ACS OMEGA

Open Access

http://pubs.acs.org/journal/acsodf

Article

Sustained-Release Microspheres of Cyclodextrin−Resveratrol Complex Using Fenugreek Galactomannan Hydrogels: A Green Approach to Phytonutrient Delivery

Umesh Kannamangalam Vijayan, Aswadh Krishna, Prasanth Shanmughan, Balu Maliakel, and Krishnakumar Illathu Madhavamenon*

Cite This: *ACS Omega* 2024, 9, 35275−35286

Read Online

ACCESS | Metrics & More | Article Recommendations | Supporting Information

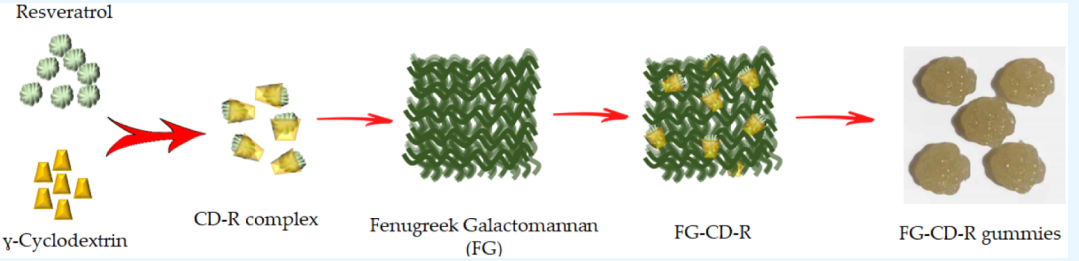

ABSTRACT: Food matrices are becoming increasingly complex with the impregnation of phytonutrients with health-beneficial pharmacological effects. Herein, we report the preparation, characterization, and functional application of soluble and stable microspheres of *trans*-resveratrol (*t*-RES) developed through a water-based green process involving cyclodextrin (CD) and fenugreek galactomannan (FG). Spectroscopic and thermodynamic calculations identified γ-CD as the best CD to form a stable cyclodextrin−resveratrol inclusion complex (CD-R, 49-fold enhanced solubility); however, it exhibited a burst release profile. The sustained release of resveratrol was achieved by further encapsulating the inclusion complex within the fenugreek galactomannan hydrogel scaffold by a gel-phase dispersion process, resulting in an amorphous powder (FG-CD-R) as evident from powder X-ray diffraction (PXRD), differential scanning calorimetry (DSC), and scanning electron microscopy (SEM) studies. Fourier transform infrared spectroscopy (FTIR) and nuclear magnetic resonance (NMR) studies confirmed the formation of the inclusion complex with no chemical alterations. When dissolved in water, FG-CD-R swelled and released stable cuboid structures with an average particle size of 500 ± 53 nm with a zeta potential of −52 ± 5.3 mV. FG-CD-R demonstrated a sustained-release profile upon in vitro release studies. Accelerated study demonstrated its stability for a shelf-life of two years. Further it was shown to be suitable for the preparation of transparent gummies with improved sensory attributes compared to unformulated *t*-RES. In summary, FG-CD-R is simple to prepare and easily scalable, providing a sustained-release *t*-RES with a natural, food-grade, and clean label status (non-genetically modified, allergen-free, vegan, and free from residual solvents) for nutritional applications.

1. INTRODUCTION

Resveratrol (3,4′,5-trihydroxy-*trans*-stilbene), a naturally occurring polyphenolic phytoalexin compound found in several plants such as grapes, berries, peanut sprouts, and herbs, is a typical example of hydrophobic and water-insoluble phytonutrients. It offers a wide spectrum of health benefits such as anticancer effect,[1] but with poor bioavailability. Resveratrol exists in two isomeric forms, namely *cis* and *trans,* in which *trans*-resveratrol (*t*-RES) is dominant and more bioactive.[1] Recently, there has been a growing interest for *t*-RES, in both the food and pharmaceutical industries due to its antioxidant, anti-inflammatory, antiglycemic, cardioprotective, neuroprotective, and anticancer properties.[2,3] However, various animal and human pharmacokinetic studies have indicated that its poor bioavailability (<1%) is a major limitation for its therapeutic and functional benefits.[4]

Low water solubility (<20 μg/mL), instability in the gastrointestinal tract, rapid biotransformation to glucuronides and sulfates, and a relatively short elimination half-life (<2 h) have been identified as the major factors limiting the bioavailability of *t*-RES.[5] A number of encapsulation technologies and vehicles have been reported to address these issues, including liposomes,[6] modified protein nanoparticles, emulsions, oleogels, micelles, and hydrogels.[7−11] Despite enhancements in solubility and bioavailability achieved

Received: December 8, 2023
Revised: May 8, 2024
Accepted: July 16, 2024
Published: August 7, 2024

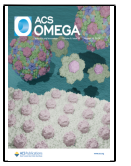

with many of these formulations, their applications in food and nutraceuticals are limited due to the extensive use of synthetic, nonfood grade surfactants. Some of the widely used synthetic emulsifiers include Cremophor EL, polysorbates, polyglycerol polyricinoleate, Labrasol, Transcutol P, etc.,[5,12,13] and polymers include cross-linked polystyrene polymers, cross-linked poly(methyl methacrylate)s, polyethylene glycol-caprolactone block copolymers, polyglycerol copolymers, lactic acid−glycolic acid copolymers, etc.[14−16] Still, there is scope for using natural food-grade polymers to develop "green" approaches in phytonutrient delivery.

Cyclodextrin (CD)-based inclusion complexes have been widely reported in both pharmaceuticals and nutraceuticals to improve solubility, stability, and bioavailability of hydrophobic compounds.[17] Cyclodextrins are cyclic oligosaccharides composed of D-glucopyranose units linked by α-(1,4) glycosidic bonds to produce CDs with 6, 7, and 8 units, commonly referred to as α-, β-, and γ-cyclodextrins respectively.[18] They are Generally Recognized as Safe (GRAS) by the Food and Drug Administration (FDA) and are approved as food ingredients in the USA, Europe, Japan, and other countries.[19] Cyclodextrins, especially β-CDs such as hydroxypropyl-β-CD and randomly methylated-β-CD, have been reported to form soluble inclusion complexes with *t*-RES. However, their bioavailability showed little improvement when ingested.[20] The reason is attributed to its rapid drug release and fast systemic clearance. Furthermore, sustained-release formulations of *t*-RES were reported to overcome the issue of burst release. Carbonyldiimidazole-cross-linked CD nanosponges showed better permeation in in vitro studies.[21] Similarly, a codelivery formulation of *t*-RES and curcumin using pyromellitic dianhydride cross-linked CD nanosponges improved permeation and anticancer activity against breast cancer cells.[22] However, such modifications find limited applications for nutrients due to the extensive usage of chemicals.

We hypothesized that impregnation of the inclusion complex within a hydrogel scaffold might modulate its release properties. Thus, in the present study, we attempted the uniform impregnation of cyclodextin−resveratrol inclusion complex (CD-R) within a soft hydrogel scaffold produced from fenugreek (*Trigonella foenum graecum*)-soluble dietary fiber (galactomannan). Here, we report our investigation into the optimized complexation of *t*-RES with various CDs (α-, β-, and γ-CDs) under varying conditions of pH and temperature and their solubility. The optimized complex was then subjected to structural, thermal, and morphological studies, with special emphasis on in vitro release, mechanism of interaction, and thermodynamics. Fluorescence studies were conducted to correlate the nature and thermodynamic parameters of the CD-R complexation. The optimized CD-R complex was further modified with fenugreek galactomannan hydrogel (FG-CD-R) to engineer sustained-release properties and to be applied as a functional food ingredient.

2. MATERIALS AND METHODS

Various grades of cyclodextrin were provided by Wacker Chemie AG (Mumbai, India). *trans*-Resveratrol (*t*-RES, 99%) was obtained as a gift sample from Akay Natural Ingredients Private Limited (Kochi, India). Pepsin and pancreatin were procured from Sigma-Aldrich (St. Louis, USA) and SRL Private Limited (Mumbai, India), respectively. All other chemicals, reagents, and solvents were of analytical grade (unless otherwise specified) and were purchased from Merck, Mumbai, India.

2.1. Selection of Suitable Cyclodextrin for Complexation of *t*-RES. Cylodextrins (α-, β-, and γ-) were screened for their complexation capacity with *t*-RES based on their respective aqueous solubility and stability under varying pH (3, 5, 7 and 9) and temperature (277, 303, 333, 343, and 353 K) conditions following a reported method.[23] About 100 μM *t*-RES standard solution was prepared in phosphate buffer and mixed with an equimolar solution of the respective CD and then homogenized. The solution pH was adjusted using 0.1 M NaOH or 0.1 M HCl, and the resulting mixture was maintained for 60 ± 5 min at room temperature and further subjected to UV/vis spectroscopy studies (Shimadzu UV-1900, UV-Probe software, Japan). The variations in absorbance with changes under reaction conditions were monitored.

2.2. Fluorescence Analysis and Thermodynamic Evaluation of the CD-R Inclusion Complex. The fluorescence spectra of the *t*-RES solution (30 μM) with varying concentrations of CD (10−40 μM) at different temperatures (298, 303, and 308 K) were analyzed using a fluorescence microplate reader (Thermo Scientific-Varioskan LUX, Skanlt Software, USA). The polarity of the test solution was maintained constant at a fixed methanol concentration (10% v/v) throughout the analysis. The excitation wavelength was maintained at 334 nm, and the emission spectra were recorded between 300 and 450 nm at 10 nm slit width. Fluorescence quenching by CD was evaluated, and the quenching constant and binding constant were determined using the Stern−Volmer equation. The Van't Hoff equation was employed to deduce the thermodynamic parameters of CD-R interactions under varying conditions, assuming that the heat capacity remains constant across the temperature range selected.[24] Thermodynamic evaluation helps to establish the nature of interaction to be more energy dependent or independent and thereby establishes the need for process parameters.

2.3. Preparation of the Fenugreek Galactomannan Hydrogel-Decorated Cyclodextrin−Resveratrol Complex (FG-CD-R). The fenugreek galactomannan hydrogel-decorated cyclodextrin−resveratrol complex (FG-CD-R) was prepared in two steps. In the first step, the inclusion complex of resveratrol with CD (CD-R) was formed, and in the second step, this complex was incorporated into the hydrogel scaffold and then dehydrated to obtain a powder.

2.3.1. Preparation of the Inclusion Complex. The cyclodextrin that exhibited the maximum complexation capacity and solubility for *t*-RES, under varying pH and temperature conditions, as discussed in section 2.1, was selected for the preparation of FG-CD-R. The complex was prepared by a modified method of Bertacche et al., where *t*-RES and CD were taken in a 2:1 molar ratio and the mixture was dispersed in water at pH of 6.8 ± 0.2 and stirred for 3 h.[25] The solution was allowed to stand for an additional 3 h and then centrifuged to remove any undissolved particles. The clear supernatant was subsequently freeze-dried to obtain CD-R powder.

2.3.2. Encapsulation of the CD-R Complex within the FG Hydrogel Scaffold. A gel-phase dispersion method was employed for the preparation of FG-CD-R. Briefly, the micronized fiber powder was uniformly dispersed in water and kept for 2 h with slow stirring. Once, the FG fibers were properly hydrated and swelled, the CD-R complex powder was

https://doi.org/10.1021/acsomega.3c09828
ACS Omega 2024, 9, 35275−35286

added and blended uniformly using a high shear homogenizer (Silverson Machines Limited, Buckinghamshire, United Kingdom). The homogeneous mass thus obtained was dried under a vacuum and powdered to form FG-CD-R.

2.3.3. Estimation of Resveratrol Content and Drug Loading Efficiency. A validated high-performance liquid chromatography (HPLC) method was used for the quantification of resveratrol content in CD-R complexes.[26] Briefly, about 50 mg of resveratrol or its complex was weighed into a standard flask and sonicated with 50 mL of methanol for 20 min. Once the solid was completely dissolved, it was made up to 100 mL with methanol, and 20 μL of this solution was injected into a HPLC fitted with a Phenomenex column (250 mm × 4.6 mm, 3 μm) and a photodiode array detector (Shimadzu LC 20 AT, Shimadzu Analytical Private Limited, Mumbai, India). The mobile phase consisting of acetonitrile (25% v/v) and acidified water (0.1% H_3PO_4) at 1 mL/min was employed for analysis. Analytical standard *t*-RES was obtained from Sigma-Aldrich, Bangalore, India (CAS no. 501-36-0).

The encapsulation efficiency of the complexes was measured by dissolving 100 mg of the respective complex in 100 mL of water and sonicating for 3 min. The solution was filtered through a syringe filter (0.45 μm), and the *t*-RES content was analyzed by HPLC. The encapsulation efficiency was then calculated using the equation:

$$\text{Encapsulation efficiency} = \frac{W_t}{W_i} \times 100$$

where W_t is the total amount of resveratrol in the complex and W_i is the total quantity of resveratrol added initially. The drug loading percentage was determined using the following equation:

$$\%\ \text{drug loading} = \frac{(\text{total drug} - \text{free drug})}{\text{weight of drug complex}} \times 100$$

2.4. Characterization of the FG-CD-R Complex. Powder samples of *t*-RES, γ-CD, fenugreek galactomannan, and the complexes CD-R and FG-CD-R were subjected to various analyses as follows. Powder X-ray diffraction (PXRD) studies were performed on a Rigaku MiniFlex Advanced instrument: target Cu, kα-1.54 Å, Filter-Ni; voltage, 40 kV; time constant, 5 min/s; scanning rate, 1°/min; a 2θ angle range of 5−90° (Rigaku, Tokyo, Japan). Attenuated total-reflectance Fourier-transform infrared spectra (ATR-FTIR) were recorded on a Thermo Nicolet iS50 spectrophotometer (Thermo fisher scientific, Madison, WI, USA). Sixty-four scans per minute, in the wavelength range of 4000−400 cm^{-1} with a resolution of 4 cm^{-1}, were taken for each sample. Differential scanning calorimetry (DSC) studies were performed on DSC 204 F1 Phoenix DSC instruments (Netzsch companies, Selb, Germany). An empty pan was used as a reference material, and samples were scanned at a rate of 10 K/min in the range of 293−573 K. The morphology of the powder samples was investigated by field emission scanning electron microscopy (FESEM) using an FESEM Joel 6390 LA equipment (JEOL Limited, Tokyo, Japan).

The solubility and particle size of the samples were evaluated as previously reported.[27] The samples of defined weight (~700 mg) were dispersed in 100 mL of deionized water and sonicated for 5 min, followed by centrifugation (3000 rpm for 10 min). The solution was then subjected to HPLC analysis to measure the soluble resveratrol content. The particle size and zeta potential of the samples were evaluated by a dynamic light scattering (DLS) method, employing Horiba SZ-100 particle size analyzer (Horiba India Private Limited, Bengaluru, India). The shape and size of the particles were evaluated with a high-resolution transmission electron microscope (HR-TEM) (JEOLJEM-2100 LaB6, Jeol Co Limited, Japan).

2.5. Swelling Studies. The swelling capacity was measured as the weight of solvent imbibed per gram of the substance. Briefly, about 1 g of the substance (FG or FG-CD-R) was placed in a preweighed 50 mL cindered silica crucible and kept for hydration in a beaker filled with water. Care was taken to keep the water level in the outer beaker and crucible the same. After 24 h, the excess water in the crucible was drained off, and the weight of the swollen substance along with the crucible was noted. From the difference in the initial and final weight of the crucible, the amount of solvent imbibed in the substance was calculated and expressed as the swelling capacity in g/g.

Swelling capacity (g/g) = weight of the solvent imbibed per gram of the substance

2.6. In Vitro Release Profiling under Gastrointestinal Conditions. An in vitro release study was performed for CD-R and FG-CD-R in simulated gastric fluid (SGF) and simulated intestinal fluid (SIF) separately. Pepsin-based SGF and pancreatin-based SIF were prepared as reported by Junaković et al.[28] The pH values of SGF and SIF were adjusted to 2 and 7 using either 1 M HCl or 1 M NaOH. To carry out the enzymatic gastrointestinal release studies, the respective samples (about 25 mg of CD-R or FG-CD-R in 5 mL of SGF or SIF) were taken in a dialysis bag and then placed in a beaker containing 100 mL of SGF or SIF. The release profile of *t*-RES was quantified by withdrawing samples at regular time intervals (0, 1, 2, 3, 4, 5, 6, 8, 10, 12, and 24 h), and the *t*-RES content was estimated.

2.7. Storage Stability. The storage stability of CD-R and FG-CD-R complexes was assessed by an accelerated stability test as per the guidelines of the International Conference of Harmonization (ICH) of technical requirements for the stability testing of new drugs and products.[29] Briefly, packets of 10 g each of the complexes, packed in double-layered polyethylene bags and a high-density polypropylene bottle with an airtight screw cap, were kept in a stability chamber (Remi, Mumbai, India) and incubated at 310 ± 2 K and 70 ± 5% relative humidity for a period of 6 months. The physicochemical properties of the sample were analyzed at intervals of 0, 1, 2, 3, and 6 months.

2.8. Preparation of Gummies and Sensory Evaluation. Pectin-based hydrocolloid gummies were prepared as per a previously reported method.[30] In this process, pectin was heated together with sugar and citric acid to melt and stirred for about 5 min. Then, the calculated quantities of *t*-RES (either unformulated or the formulation FG-CD-R) were added and mixed well to homogeneity. The blend was then poured into a silicon mold and kept under refrigeration conditions (~279 ± 2 K) for a period of 24 h before performing sensory analysis. Each gummy was weighed, and its *t*-RES content was estimated by HPLC.

Sensory evaluation for the gummies was performed by a sensory panel consisting of 10 members (6 males and 4 females) from Akay Natural Ingredients Private Limited, Kochi, India. Each panelist was provided with two gummies (unformulated and formulated) coded neutrally, along with response sheets (temperature ~301 ± 2 K). Panelists were

https://doi.org/10.1021/acsomega.3c09828
ACS Omega 2024, 9, 35275−35286

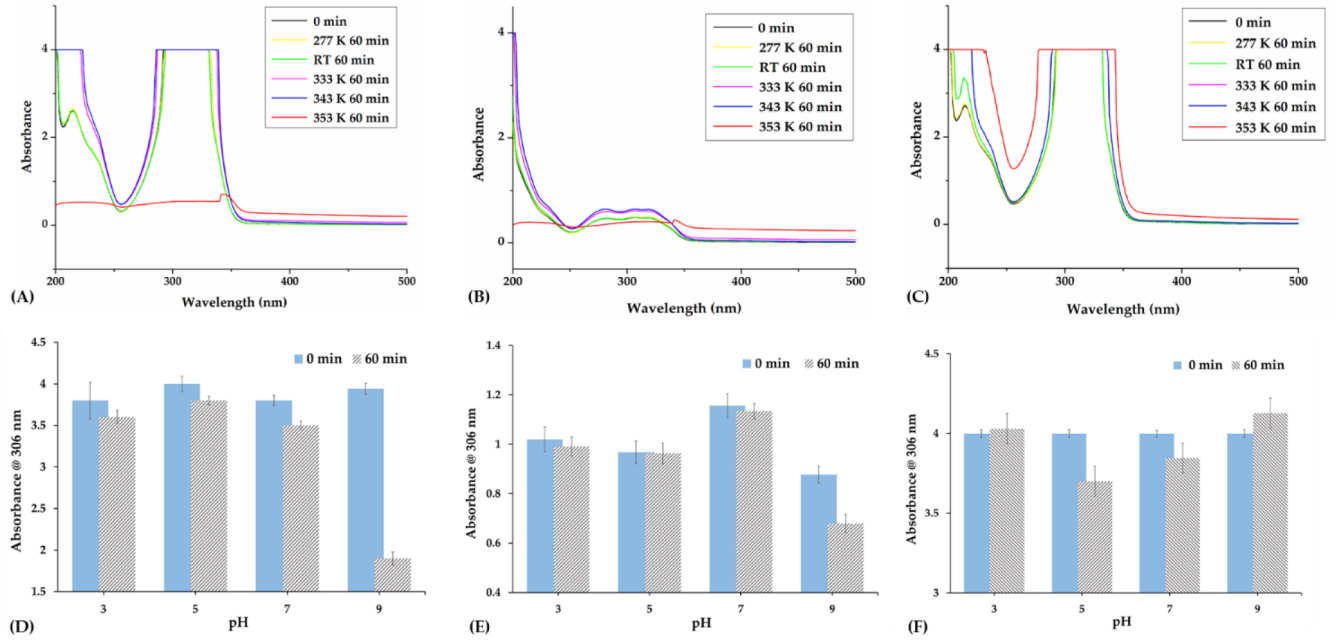

Figure 1. Spectral scan data of *t*-RES under varying temperature conditions with (A) α-CD, (B) β-CD, (C) γ-CD. (D,E,F) represent the variation in absorbance as a function of pH (3, 5, 7, and 9) for α-CD, β-CD, and γ-CD, respectively, at 306 nm.

provided with drinking water to clear their palates after each sampling. The sensory evaluations included the odor or aroma, color, taste, aftertaste, mouthfeel, and overall acceptability of the gummies using a nine-point hedonic scale (9 = like extremely, 8 = like very much, 7 = like moderately, 6 = like slightly, 5 = neither like nor dislike, 4 = dislike slightly, 3 = dislike moderately, 2 = dislike very much, 1 = dislike extremely).[31]

3. RESULTS AND DISCUSSION

Sustained-release or controlled-release formulation of a drug may be described as a programmed slow-release form, which can affect the drug release over an extended period of time. Typical sustained-release formulations provide an immediate release of a therapeutically significant concentration into the blood, followed by a gradual release of additional amounts of the drug to maintain the effect over a predetermined period.[32] It helps single dose administration instead of multiple doses, maintaining a constant systemic concentration of the drug. Sustained-release formulations are useful for molecules that are insoluble and undergo rapid metabolism to inactive metabolites.[33] In nutritional therapy, such formulations are highly favored since most phytonutrients are hydrophobic and insoluble, with poor bioavailability and rapid biotransformation. Herein, we explored the possibility of a sustained-release formulation of *t*-RES employing natural food-grade biopolymers, cyclodextrin, and galactomannan dietary fiber extracted from fenugreek. Typically, inert, biodegradable, and biocompatible synthetic polymers are used for the sustained release of drugs. Fenugreek-soluble dietary fiber provides a natural and cheap alternative to synthetic polymers and adds additional value to the formulations owing to its prebiotic potential and antihyperglycemic/antilipidemic properties.[34]

3.1. Selection of Cyclodextrin for *t*-RES Complexation. α-, β-, and γ-Cyclodextrins vary in the number of carbohydrate moieties and, consequently, in their cavity size.[35] As a result, different molecules have varying affinities towards CDs, leading to different loading levels and stability. In the present study, we followed UV−vis spectroscopic investigations under varying conditions of temperature and pH to find the best suitable CD for *t*-RES. It was found that the α-CD inclusion complex with *t*-RES exhibited good thermal stability up to 343 K (blue line in Figure 1A,B), with a red flat line at 353 K (Figure 1A,B) indicating degradation. A similar trend was observed for the β-CD-R complex at 353 K (red flat line, Figure 1B). However, the γ-CD-R complex remained stable under all the tested temperature conditions, with a λ_{max} at 306 nm (Figure 1C). Both positive and negative correlations between stability and temperature have been reported for CD complexes of hydrophobic molecules. While fatty acid-CD complexes, such as linoleic acid−β-CD, showed a positive correlation with increasing temperature,[36] methyl jasmonite and piceatannol demonstrated dissociation of the complex with increasing temperature.[37]

The stability of CD-R complexes under different pH conditions was also investigated by UV−vis spectroscopy (Figure 1D−F). The complexes of α-, β-, and γ-CDs with *t*-RES were stable under acidic conditions, but a significant reduction in absorbance at 306 nm was observed for α- and β-CDs under alkaline conditions. γ-CD, on the contrary, showed no degradation under both acidic and alkaline conditions. Our results were in agreement with those of Zupančič et al. who have reported high degradation of *t*-RES at pH higher than 6.8.[38] The stability of γ-CD-R under alkaline conditions shows the efficiency of encapsulation of *t*-RES with γ-CD. In summary, the γ-CD−R complex showed the maximum solubility and stability under given conditions. The reason for the higher stability was attributed to the effective encapsulation of the molecules inside the cavities of CDs, and possibly the stabilization via hydrophobic interactions between the host and guest.[39]

3.2. Fluorescence Analysis and Thermodynamic Evaluation of CD-R Complexation. The fluorescence spectra of *t*-RES solution containing varying concentrations

https://doi.org/10.1021/acsomega.3c09828
ACS Omega 2024, 9, 35275−35286

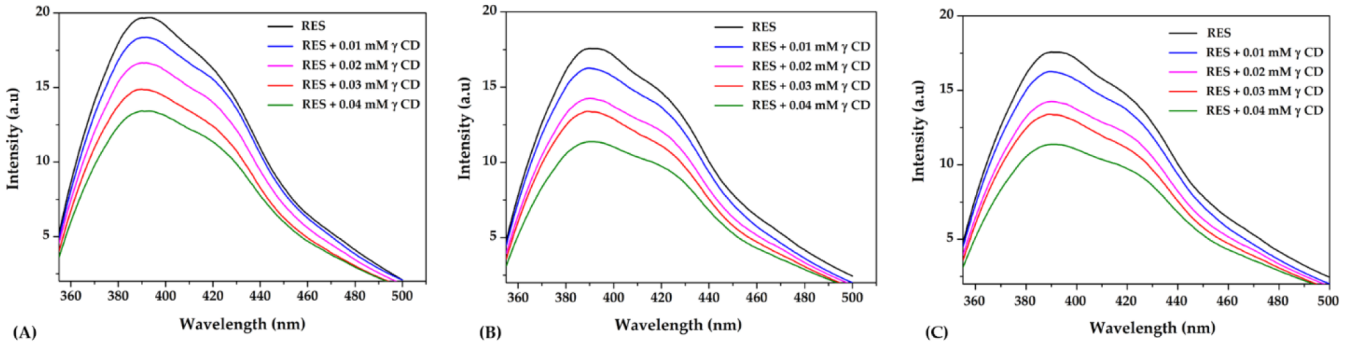

Figure 2. Fluorescence spectra of *t*-RES with different concentrations of γ-CD at (A) 298 K, (B) 303 K, and (C) 308 K.

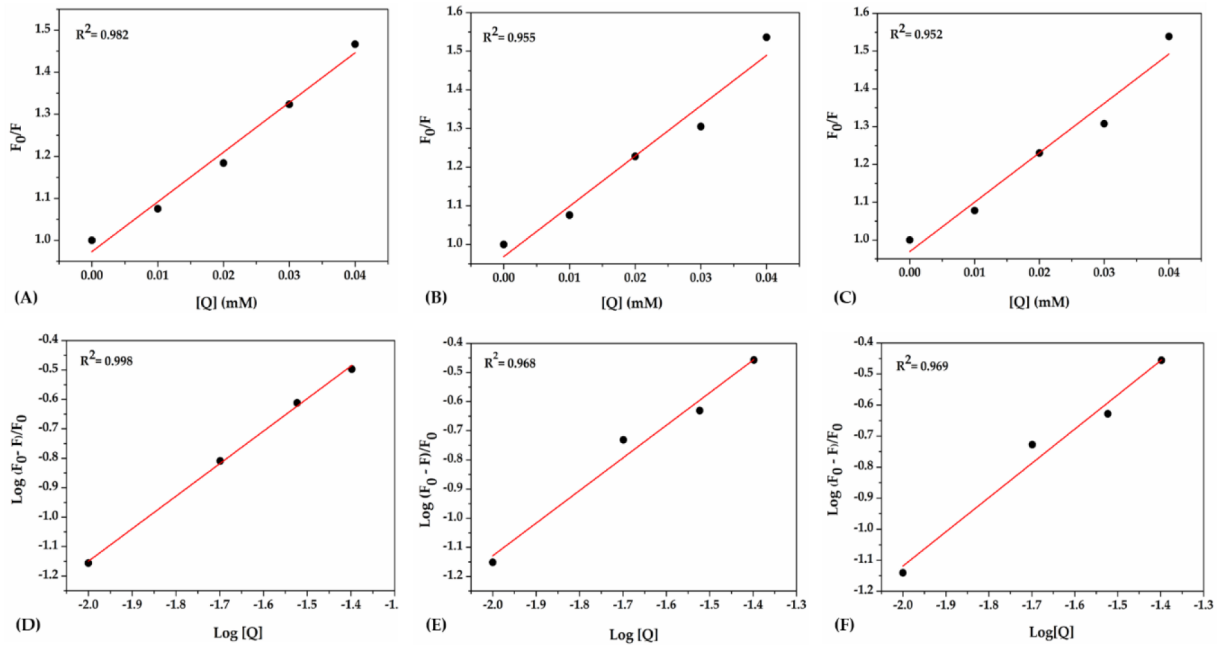

Figure 3. S−V plot of *t*-RES with γ-CD under three temperature conditions (A) 298 K, (B) 303 K, and (C) 308 K. (D,E,F) represent the double logarithmic plots of γ-CD-R complex under the same conditions.

Table 1. Quenching Constant, Binding Constant, Number of Binding Sites, and Thermodynamic Parameters of γ-CD and *t*-RES

temperature (K)	K_{sv} (L mol^{-1})	K_a (L mol^{-1})	n	ΔG (kJ mol^{-1})	ΔH (kJ mol^{-1})	ΔS (J mol^{-1} K^{-1})
298	1.182×10^4	1.149×10^3	1.2	−17.459	166.75	2.49
303	1.301×10^4	1.118×10^3	1.2	−17.683		
308	1.307×10^4	1.102×10^3	1.2	−17.937		

of γ-CD at three different temperatures (298, 303, and 308 K) were recorded at an excitation wavelength of 340 nm (Figure 2A−C). While *t*-RES solution exhibited an emission maximum at 392 nm, the fluorescence intensity decreased with increase in γ-CD concentration. No emission wavelength was observed. The quenching of resveratrol fluorescence by γ-CD was then analyzed using the Stern−Volmer equation as given below, to provide an insight into the quenching mechanism.[40]

$$\frac{F_0}{F} = nK_{sv}[Q]$$

Here, F_0 and F are the fluorescence intensities in the absence and presence of γ-CD, respectively. K_{sv} is the quenching constant, and [Q] is the concentration of γ-CD. The value of K_{sv} was determined by the slope of the plot between $\frac{F_0}{F}$ and [Q] (Figure 3A−C). It was observed that the quenching constant increases with an increase in temperature from 298 to 308 K, and the increase in K_{sv} was significant from 298 to 303 K (Table 1). This indicates that the complex formation follows a dynamic quenching pattern as K_{sv} increases with an increase in temperature.

In order to estimate the binding constant (K_a) and the number of binding sites (n), the following equation was used.

$$\log\frac{F_0 - F}{F_0} = \log K_a + n \log[Q]$$

K_a and "n" were determined from the slope and intercept of the double logarithm regression curve of $\log\frac{F_0 - F}{F_0}$ versus $\log[Q]$ based on the equation given before (Figure 3D−F).

https://doi.org/10.1021/acsomega.3c09828
ACS Omega 2024, 9, 35275−35286

Furthermore, the thermodynamic parameters [enthalpy change (ΔH) and entropy change (ΔS)] associated with the binding were determined using the Van't Hoff equation (Table 1).

$$\log K_a = \frac{-\Delta H}{2.303RT} + \frac{\Delta S}{2.303R}$$

The values of ΔH and ΔS were calculated from the slope and intercept of the plot between $1/T$ and $\ln K_a$ (Figure S1). Gibbs free energies (ΔG) were calculated based on the following equation:

$$\Delta G = -RT \ln K_a$$

The calculated values of the quenching constant (K_{sv}), binding constant (K_a), number of binding sites (n), and the thermodynamic parameters are given in Table 1. The negative value of ΔG indicated that the complexation between *t*-RES and γ-CD is spontaneous.[41] ΔH and ΔS were 166.75 kJ mol^{-1} and 2.49 J mol^{-1} K^{-1} respectively. Positive values of ΔH and ΔS concluded that the inclusion complex (γ-CD-R) is relatively hydrophobic,[42] with hydrophobic interactions binding *t*-RES in the cavities of γ-CD, which is relatively nonpolar in nature.

3.3. Preparation and Characterization of CD-R and FG-CD-R Complexes. From the above studies, we concluded that γ-CD would be the best host molecule for the guest *t*-RES to form a CD-R inclusion complex. However, CD-R is water soluble and causes a burst release once it comes in contact with water or gastrointestinal fluid. We hypothesized that surface modification or impregnation of CD-R complexes within a hydrogel scaffold would be effective in engineering sustained-release properties under gastrointestinal conditions. In this regard, we selected fenugreek galactomannan, a soluble dietary fiber, often known as fenugreek mucilage, as a soft hydrogel scaffold. Recent studies have shown that fenugreek galactomannan can be used to generate hybrid-hydrogels such as surface-modified liposomes, or for the encapsulation of micelles or emulsions of active molecules to improve their bioavailability.[26,27,43]

We prepared the CD-R complex containing 18.6% (w/w) *t*-RES and encapsulated them in the fenugreek galactomannan hydrogel scaffold in the powder form (FG-CD-R), with a *t*-RES content of 17% (w/w) (Table 2). FTIR and NMR studies were primarily conducted on the powder samples of CD-R and FG-CD-R to confirm complex formation.

Table 2. Encapsulation Efficiency, Loading Efficiency, and Particle Size

formulation	RES loading (%)	encapsulation efficiency (%)	particle size (nm)	zeta potential (mV)
CD-R	18.6%	93.0%	420 ± 34	−59.8 ± 4.6
FG-CD-R	17.0%	85.0%	500 ± 53	−52.0 ± 5.3

Molecular evidence for the formation of the inclusion complex of *t*-RES with γ-CD and their impregnation in the hydrogel scaffold to form FG-CD-R was studied by ^{1}H NMR (Figure 4). The differences in the chemical shift of *t*-RES upon complexation with γ-CD were calculated using the equation $\Delta\delta = \delta_{CD+Res} - \delta_{Res}$, where δ_{CD+Res} is the chemical shift of the CD-R complex and δ_{Res} is the chemical shift of *t*-RES (Table 3). The positive and negative values indicated the upfield and downfield shifts, respectively, which can provide information about the variations in the electronic environment of protons and hence the orientation of *t*-RES molecules in the CD cavities.[44] It was observed that the chemical shifts of H1, H2, H3, and H4 are far more affected and H6 was less shifted. Therefore, it can be concluded that H1, H2, H3, and H4 are located inside the cavity of γ-CD and H6 is located on the rim of the cavity ring of γ-CD.[45] The downfield shifts in *t*-RES can be attributed to the variations in the local polarity due to the inclusion in γ-CD.[46] Thus, the observations are consistent with inclusion complex formation. After the incorporation of CD-R into the fenugreek galactomannan hydrogel, no significant chemical shift was observed for *t*-RES. This could be due to the successful inclusion complex formation of *t*-RES with γ-CD and, hence, the subsequent surface modification with FG did not contribute to its chemical shift.

Figure 5A shows the FTIR spectra of *t*-RES, γ-CD, CD-R, and FG-CD-R. The characteristic peaks of *t*-RES were identified at 3182, 1604, and 1582 cm^{-1} corresponding to O−H stretching, C−C aromatic double bond stretching, and C−C olefinic stretching, respectively. The peak at 1379 cm^{-1} was attributed to C−O stretching, and the one at 963 cm^{-1} confirmed the *trans*-olefinic bond.[47] For γ-CD, the O−H stretching vibration was observed at 3266 cm^{-1} and the peak at 2927 cm^{-1} corresponded to C−H stretching vibrations. The asymmetric C−O−C stretching vibration and C−C/C-O vibrations were observed at around 1020−1200 per cm.[48] In CD-R, however, most of these characteristic peaks of *t*-RES were found to disappear due to the formation of the inclusion complex. The complex formation would reduce the bending and stretching vibrations.[49] In FG, the O−H stretching vibration was observed at around 3300−3700 cm^{-1}.[50] The bands observed at 2922 and 1024 cm^{-1} were attributed to the C−H and C−O stretching vibrations, respectively, and are characteristic of polysaccharides.[51] The peak around 1652 cm^{-1} can be attributed to the amide linkage originated from the proteins in the fenugreek hydrogel.[52] Furthermore, the bands around 800−820 and 872 cm^{-1} were associated with the occurrence of anomeric configurations (C−H oscillations of α and β conformers) and glycosidic linkages, attributed to α-D-galactopyranose units and β-D-mannopyranose units, respectively.[53] For FG-CD−R, the peaks of γ-CD and *t*-RES were absent and the peaks of FG were shifted. The most significant shift was observed for the amide band (1652 cm^{-1} → 1607 cm^{-1}), probably due to hydrogen bonding between the −OH groups of γ-CD and the amide bonds in the hydrogel. The absence of the characteristic peaks of γ-CD and *t*-RES further confirms the formation of the inclusion complex.

The solid inclusion complexation and its subsequent encapsulation within the fenugreek galactomannan hydrogel scaffold were also confirmed by PXRD, DSC, and SEM analyses. Figure 5B shows the PXRD spectra of *t*-RES, γ-CD, CD-R, and FG-CD-R at 2θ values from 5° to 90°. Sharp and intense diffraction peaks at 2θ values 6.6°, 16.5°, 19°, 22.4°, 23.8°, and 28.5° indicated the crystalline nature of *t*-RES,[26] and those of γ-CD was observed at 5.4°, 12.4°, 15.5°, 16.7°, 19.01°, and 21.8° confirming its cage-like crystalline nature, as previously reported.[54] In the CD-R complex, the characteristic peaks of *t*-RES were found to be absent, indicating its inclusion into the cavities of γ-CD. A previous report has also showed the absence of sharp peaks as the indication of the encapsulation efficiency.[55] The PXRD spectrum of fenugreek galactomannan showed a broad peak at around 22°, indicating its amorphous nature. FG-CD-R also exhibited a characteristic

https://doi.org/10.1021/acsomega.3c09828
ACS Omega 2024, 9, 35275−35286

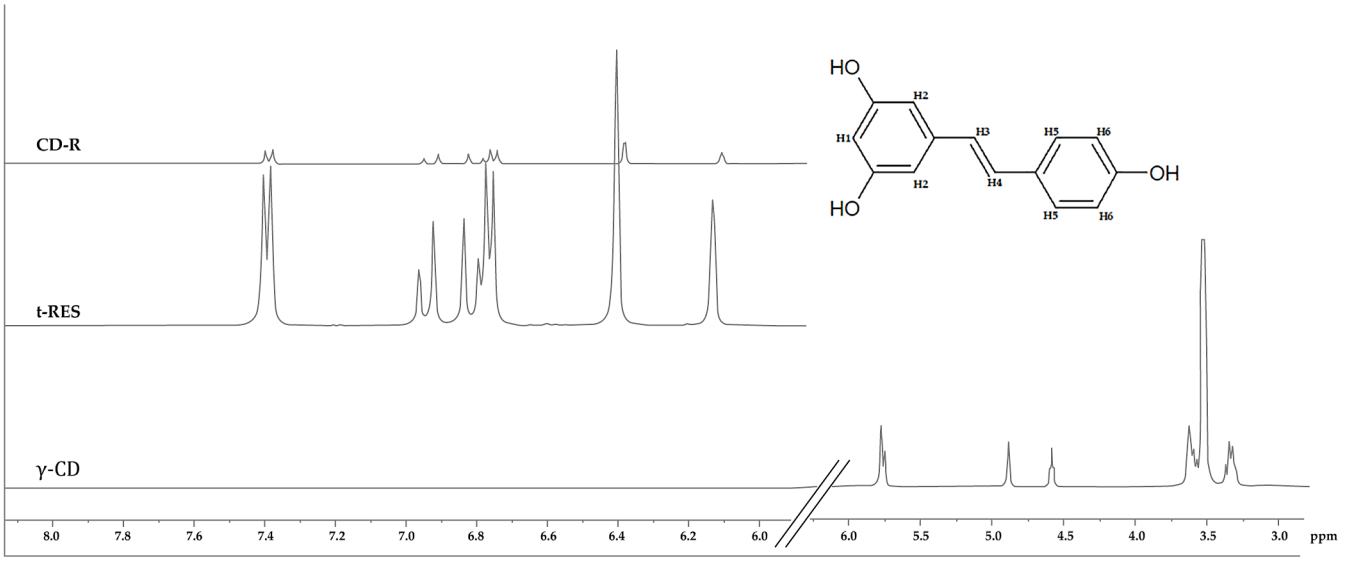

Figure 4. ^{1}H NMR spectra of *t*-RES and its complexes.

Table 3. Chemical Shift δ (ppm) of *t*-RES and CD-R Complex

	chemical shift δ (ppm)		
proton	*t*-RES	CD-R	$\Delta\delta$
H1	6.106	6.132	−0.026
H2	6.384	6.404	−0.020
H3	6.908	6.922	−0.014
H4	6.822	6.836	−0.014
H5	7.376	7.382	−0.006
H6	6.762	6.773	−0.011

pattern of amorphous nature, raised from the complete inclusion of the CD-R complex within the galactomannan hydrogel network. Such a pattern change has also been reported with resveratrol and quercetin when engulfed into hydrogel matrix.[27,43]

The DSC thermograms of *t*-RES, γ-CD, CD−R, and FG-CD-R were obtained (Figure S2). *trans*-Resveratrol showed a sharp endotherm at 540 K indicating its melting point, and γ-CD exhibited endothermic peaks at 370 and 386 K due to the absorbed moisture loss. However, the sharp endothermic peak of *t*-RES was found to be missed in the CD-R complex, and the exothermic peaks of γ-CD was shifted from 370 to 317.65 K. The peaks were also broadened indicating the encapsulation of resveratrol in the cavities of γ-CD.[56,57] DSC thermogram of FG-CD-R showed a similar trend as that of CD-R, with the absence of the exothermic peak at 540 K, indicating the complete encapsulation of CD-R in the hydrogel matrix. Such changes have already been identified as the characteristic features of inclusion complex formation and its encapsulation in the hydrogel scaffold.[26]

The morphology of *t*-RES, γ-CD, FG, CD-R, and FG-CD-R powder was studied using SEM analysis (Figure 6). *trans*-Resveratrol and γ-CD revealed a crystalline structure with sharp edges and irregular morphology. Fenugreek galactomannan, on the contrary, showed a porous structure with amorphous nature. Furthermore, the CD-R complex showed a

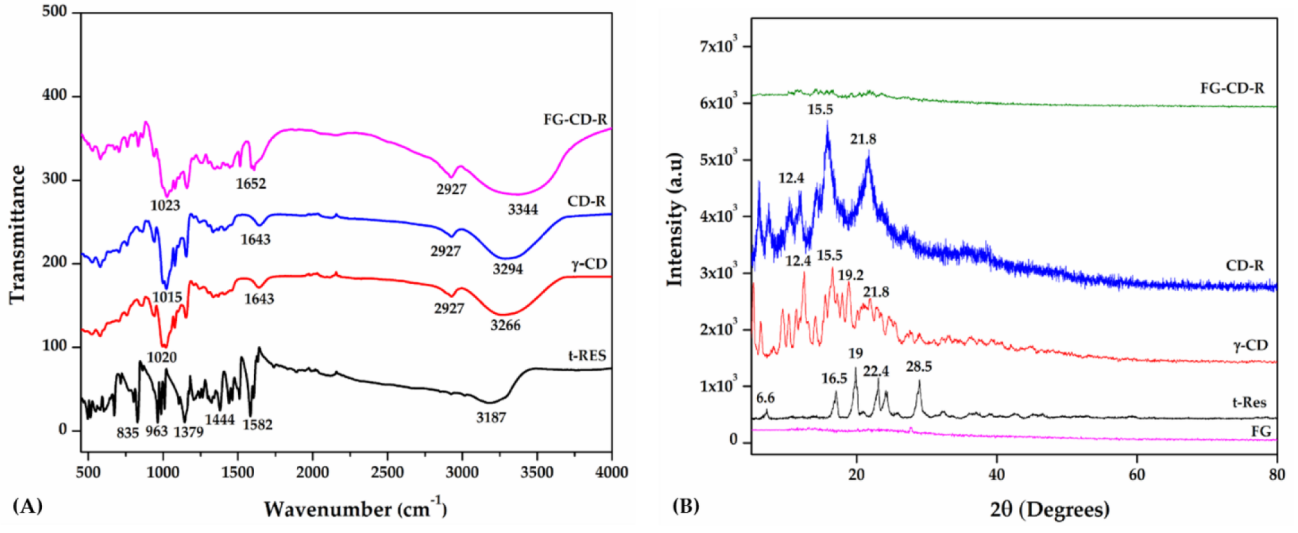

Figure 5. Characterization of *t*-RES and its complexes: (A) FTIR spectra and (B) PXRD

https://doi.org/10.1021/acsomega.3c09828
ACS Omega 2024, 9, 35275−35286

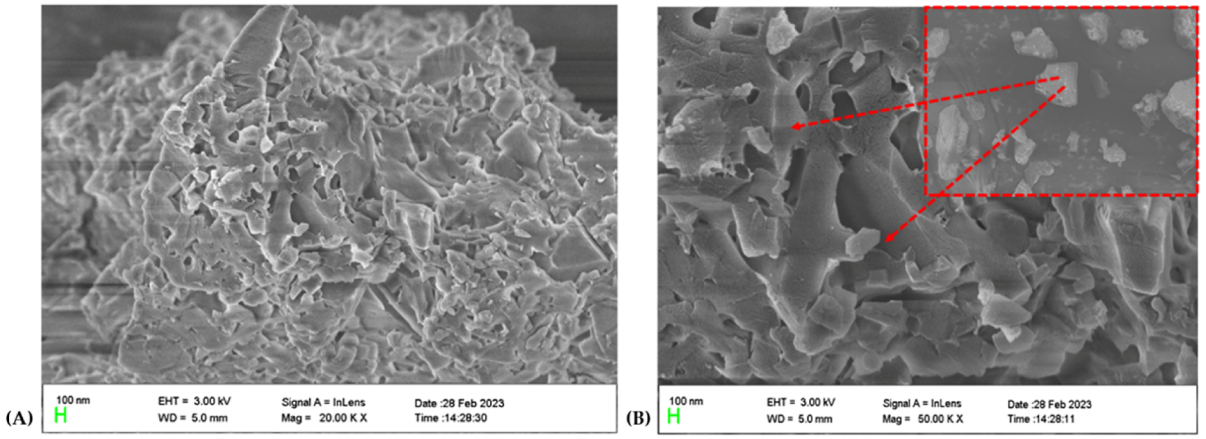

Figure 6. FESEM images of (A) FG and (B) FG-CD-R; inset: magnified image of FG-CD-R indicating the cuboid clustering.

highly organized rectangular structure indicating the inclusion of *t*-RES into the cavities of γ-CD. In the case of FG-CD-R complex, an amorphous pattern with inclusion of CD-R complexes within the pores of hydrogel scaffold was evident.

trans-Resveratrol is an insoluble molecule with a solubility of around 21 μg/mL. γ-CD, on the contrary, is water soluble (18 mg/mL). Upon complexation, the solubility of resveratrol was found to be increased 49 times (1024.3 μg/mL, Figure 7A).

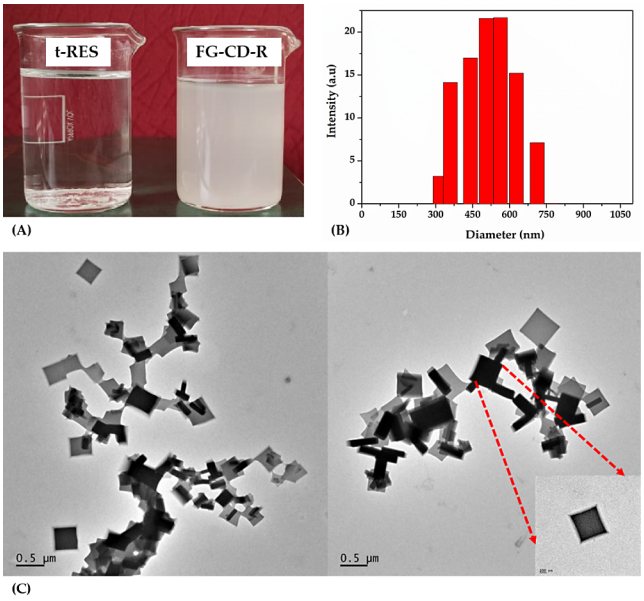

Figure 7. (A) Photograph of *t*-RES and FG-CD-R indicating their solubility, (B) hydrodynamic size distribution of FG-CD-R in aqueous solution, and (C) TEM image of FG-CD-R complex showing the cuboid particles (inset).

Further encapsulation of CD-R by the hydrogel, decreased the instant solubility of CD-R, but there was no apparent reduction in the solubility. This could be due to the lag time for the uniform dispersion of the FG-CD-R particles to swell in the solution.

The average particle size of the CD-R complex was around 420 ± 34 nm with a zeta potential of −59.8 ± 4.6 mV, and that of FG-CD-R was 500 ± 53 nm (Figure 7B, zeta potential, −52 ± 5.3 mV). The increased particle size and zeta potential of FG-CD-R may be attributed to the entrapment of the inclusion complex in the hydrogel matrix, which resulted in enhanced stability. Furthermore, TEM analysis showed a cuboid structure for the CD-R complex in the solution (Figure 7C). This type of cuboid structures signifies a high loading efficiency for the delivery of carrier candidates.[58]

3.4. Swelling Studies. The swelling capacity of a polymer gives a measure of the amount of a particular solvent it can hold when it comes in contact. The swelling capacity in water decides the water holding capacity and stability of a hydrogel. The release of a trapped molecule from a hydrogel network is mainly caused by diffusion, and the swelling index significantly contributes to it.[59] It was observed that the soluble FG fiber matrix absorbed 23.1 g of water per gram of fiber, indicating a swelling capacity of 23.1 g/g. When CD-R complexes were incorporated into the FG hydrogel matrix, the swelling capacity was found to be reduced to 3.5 g/g. The reduction in the swelling capacity was found to be dependent on the amount of fiber since FG-CD-R contains only 10% (w/w).

3.5. In Vitro Release Profiling under Gastrointestinal Conditions. The release profile of *t*-RES in the gastrointestinal tract was evaluated by using in vitro SGF and SIF models. It has been observed that *t*-RES in CD-R released at a faster rate compared to FG-CD-R under both SGF and SIF conditions. After 24 h of incubation in SGF, the release of *t*-RES was found to be >80% within 5 h for CD-R. However, FG-CD-R showed about only 20% release in 5 h and 60% in 24 h (Figure 8A). Also under SIF conditions, the percentage release of *t*-RES from CD-R and FG-CD-R was about 70% and 20%, respectively, within 5 h. The percentage release was only about 60% after 24 h (Figure 8B). A previous report using hydroxypropyl-βCD also reported a similar release profile indicating the burst release as a characteristic feature of the inclusion complex with CDs.[60] However, the addition of polymers such as poly(methyl methacrylate) (PMMA) and poly(lactic-*co*-glycolic acid) (PLGA) to the β-cyclodextrin complex of sulfadiazine sodium salt resulted in a slow release, similar to what was observed with FG-CD-R.[61] Thus, our results demonstrate the potential of using natural prebiotic fibers, such as FG, as alternatives to synthetic polymers for sustained release, for the first time.

3.6. Storage Stability. FG-CD-R complexes showed good stability and a shelf life of more than 2 years when subjected to accelerated stability studies as per ICH guidelines, indicating the suitability for commercial production and storage as a functional ingredient (Table 4).

https://doi.org/10.1021/acsomega.3c09828
ACS Omega 2024, 9, 35275−35286

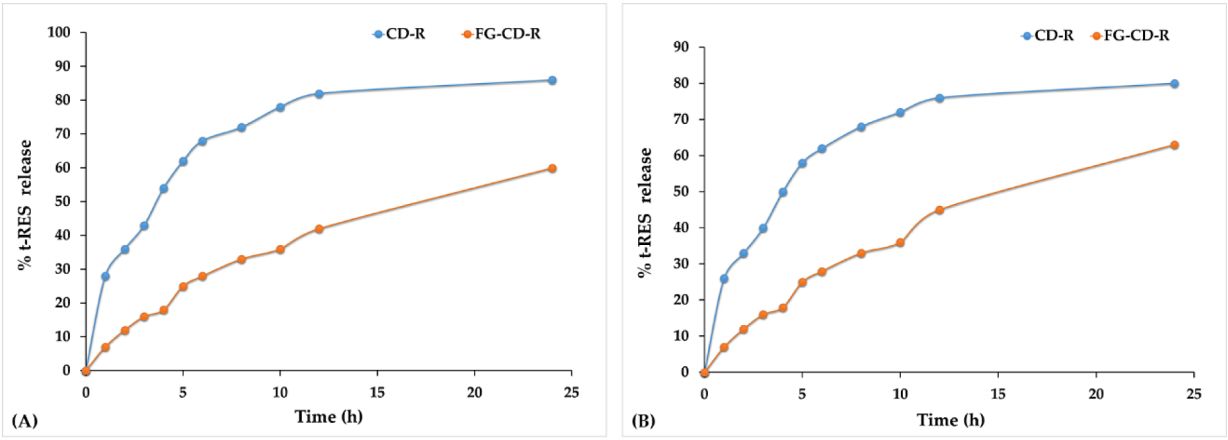

Figure 8. In vitro drug release profile in (A) simulated gastric fluid and (B) simulated intestine fluid.

Table 4. Stability Data under Accelerated Conditions (313 ± 2 K and 70 ± 5% Relative Humidity)

formulations	months	RES content (%)	particle size (nm)	zeta potential (mV)
CD-R	0	100.2 ± 1.4	420 ± 34	−59.8 ± 4.6
	1	99.9 ± 1.7	432 ± 42	−60.8 ± 4.2
	2	99.2 ± 1.2	440 ± 38	−61.8 ± 3.6
	3	98.9 ± 1.6	483 ± 26	−59.6 ± 3.3
	6	93.4 ± 1.3	453 ± 33	−59.8 ± 3.7
FG-CD-R	0	99.9 ± 1.3	500 ± 52	−54.0 ± 4.4
	1	99.9 ± 0.8	498 ± 36	−53.4 ± 5.2
	2	99.4 ± 1.1	522 ± 54	−52.6 ± 3.8
	3	99.6 ± 0.9	568 ± 26	−53.8 ± 5.6
	6	99.1 ± 0.8	546 ± 43	−53.0 ± 5.3

3.7. FG-CD-R as a Functional Food Ingredient.

Pectin and gelatin gummies have recently emerged as a preferred food delivery format for micronutrients and phytonutrients.[30] However, their poor solubility and instability under processing conditions limit the application of many vitamins and phytonutrients in gummies. Moreover, the sensory attributes of the nutrients present serious challenges for incorporating pharmacologically relevant doses into gummies. We prepared pectin gummies containing approximately 25 mg of *t*-RES/gummy, using both unformulated *t*-RES and formulated FG-CD-R. It was found that using FG-CD-R for gummy preparation was relatively easy compared to unformulated *t*-RES and resulted in transparent and stable gummies. Upon sensory evaluation, FG-CD-R gummies stood significantly better than the unformulated *t*-RES due to the effective masking of bitterness and astringency (Figure 9).

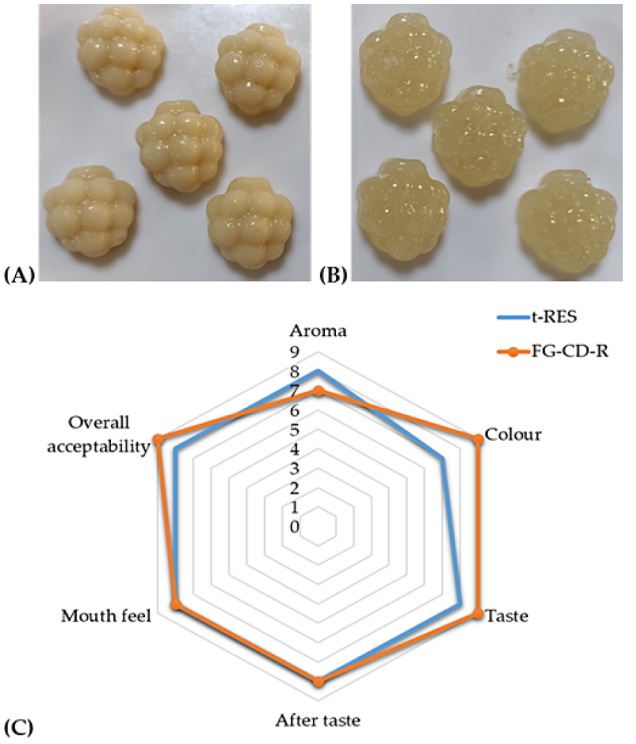

Figure 9. Gummies prepared from (A) unformulated *t*-RES and (B) FG-CD-R. (C) Sensory evaluation results based on the nine hedonic scale score.

The aforementioned results clearly demonstrated the possibility of producing stable and soluble *t*-RES inclusion complexes with CDs, especially at relatively high concentrations of 15 to 20% (w/w), which are relevant for therapeutic dosage forms. Furthermore, encapsulating *t*-RES into a hydrogel scaffold was found to be effective in engineering sustained-release properties. At suitable dilutions, FG can hold water to form a gel, and the microstructure of the gel enables the encapsulation of hydrophobic molecules and oils within its conformationally directed hydrophobic pockets created by the swollen network. Once dehydrated, such hydrogels can be converted to a powder form and rehydrated to revert to hydrogel, indicating its reversible nature. The hydrogel scaffold helps in minimizing taste and maintaining stability under high-temperature conditions for functional food applications. This is clear from the sensory evaluation of the gummies and sachets prepared in this study. Upon consumption, the hydrogel swells in the gastrointestinal fluid, and the mucoadhesive nature of FG enables it to tightly bind to the microvilli (small finger-like structures) of the intestinal epithelial membrane, leading to the sustained release of soluble *t*-RES for better absorption and bioavailability. Mucoadhesive polymers are well known for improving residence time in the GIT by interacting with the structures of the microvilli. In contrast, unformulated *t*-RES is a hydrophobic and water-insoluble molecule that is incompatible with gastrointestinal fluid, resulting in poor bioavailability. Future studies are recommended to evaluate the pharmacokinetics and efficacy of these formulations under in vivo conditions to understand the effects of these modifications.

https://doi.org/10.1021/acsomega.3c09828
ACS Omega 2024, 9, 35275−35286

4. CONCLUSIONS

In summary, this study aimed to develop water-soluble, sustained-release microspheres for hydrophobic and insoluble phytonutrients such as *trans*-resveratrol having poor oral bioavailability by following a green approach (employing natural and food-grade excipients and water-based process). Such formulations find wide applications in food, nutraceuticals, and dietary supplements. We found that γ-CD has the best complexation ability with *t*-RES. We then developed an aqueous process for stable loading of *t*-RES into the cavities to form a CD-R inclusion complex. We further established the encapsulation of inclusion complexes within a fenugreek galactomannan hydrogel scaffold, which was then dehydrated to produce a free-flowing powder (FG-CD-R). Spectroscopic studies and thermodynamic calculations revealed the hydrophobic interactions, stability, and spontaneous formation of the complex. Additional characterization using FTIR, NMR, PXRD, DSC, and TEM revealed that FG-CD-R is an amorphous, stable, water-soluble, and reversible hydrogel powder. When dissolved in water, it formed stable cuboid particles approximately 500 nm size (as evident from DLS and TEM studies), indicating high loading efficiency. A 49-fold enhancement in the solubility of *t*-RES was observed upon formulation and showed a sustained-release profile under in vitro gastrointestinal conditions. It was found to be stable at 353 K and provided an easy way for the preparation of stable and transparent gummies with improved sensory attributes. Additionally, the process was scalable and yielded natural, food-grade, clean label (nongenetically modified, allergen-free, vegan, and residual solvent-free) formulations with sustained-release properties suitable for nutritional applications.

■ ASSOCIATED CONTENT

Supporting Information

The Supporting Information is available free of charge at https://pubs.acs.org/doi/10.1021/acsomega.3c09828.

Plot of ln K_a verse $1/T$ (Figure S1); DSC thermogram (Figure S2) (PDF)

■ AUTHOR INFORMATION

Corresponding Author

Krishnakumar Illathu Madhavamenon − *R&D Centre, Akay Natural Ingredients, Kochi, Kerala 683561, India;* orcid.org/0000-0003-0594-7650; Email: krishnakumar.im@akay-group.com

Authors

Umesh Kannamangalam Vijayan − *R&D Centre, Akay Natural Ingredients, Kochi, Kerala 683561, India*

Aswadh Krishna − *School of Physical Sciences, Amrita Vishwa Vidyapeetham, Coimbatore 641112, India*

Prasanth Shanmughan − *R&D Centre, Akay Natural Ingredients, Kochi, Kerala 683561, India*

Balu Maliakel − *R&D Centre, Akay Natural Ingredients, Kochi, Kerala 683561, India*

Complete contact information is available at: https://pubs.acs.org/10.1021/acsomega.3c09828

Author Contributions

K.I.M. is the principal investigator who supervised the project and reviewed the manuscript. A.K. conducted the formulation trials and developed the manuscript along with U.K.V. P.S. performed the characterization, and B.M. arranged the funding and reviewed the manuscript.

Notes

The authors declare no competing financial interest.

■ ACKNOWLEDGMENTS

The authors thank Sophisticated test and instrumentation centres at the Cochin University of Science and Technology, Kerala, India, and Mahatma Gandhi University, Kerala, India for physicochemical characterization. A. K. expresses his sincere thanks to both Amrita School of Physical Sciences for the permission for the project work as part of the curriculum for postgraduate course in Chemistry and to the R&D of Akay Natural Ingredients for the permission and guidance to work. Authors also thank Mr Ashil Joseph and Ms Midhu Varghese at the R&D Akay for the analytical support and Mr Pearl Kanneth for gummy preparation.

■ REFERENCES

(1) Anisimova, N. Y. U.; Kiselevsky, M. V.; Sosnov, A. V.; Sadovnikov, S. V.; Stankov, I. N.; Gakh, A. A. Trans-, cis-, and dihydro-resveratrol: A comparative study. *Chem. Cent. J.* **2011**, *5* (1), 88.

(2) Cheng, C. K.; Luo, J. Y.; Lau, C. W.; Chen, Z. Y.; Tian, X. Y.; Huang, Y. Pharmacological basis and new insights of resveratrol action in the cardiovascular system. *Br. J. Pharmacol.* **2020**, *177* (6), 1258−1277.

(3) Farhan, M.; Rizvi, A. The Pharmacological Properties of Red Grape Polyphenol Resveratrol: Clinical Trials and Obstacles in Drug Development. *Nutrients* **2023**, *15* (20), 4486.

(4) Kapetanovic, I. M.; Muzzio, M.; Huang, Z.; Thompson, T. N.; McCormick, D. L. Pharmacokinetics, oral bioavailability, and metabolic profile of resveratrol and its dimethylether analog, pterostilbene, in rats. *Cancer Chemother. Pharmacol.* **2011**, *68* (3), 593−601.

(5) Yen, C.-C.; Chang, C.-W.; Hsu, M.-C.; Wu, Y.-T. Self-Nanoemulsifying Drug Delivery System for Resveratrol: Enhanced Oral Bioavailability and Reduced Physical Fatigue in Rats. *Int. J. Mol. Sci.* **2017**, *18* (9), 1853.

(6) Xu, X.; Tian, M.; Deng, L.; Jiang, H.; Han, J.; Zhen, C.; Huang, L.; Liu, W.; et al. Structural degradation and uptake of resveratrol-encapsulated liposomes using an in vitro digestion combined with Caco-2 cell absorption model. *Food Chem.* **2023**, *403*, 133943.

(7) Li, W.; Bi, D.; Yi, J.; Yao, L.; Cao, J.; Yang, P.; Li, M.; Wu, Y.; Xu, H.; Hu, Z.; Xu, X.; et al. Soy protein isolate-polyguluronate nanoparticles loaded with resveratrol for effective treatment of colitis. *Food Chem.* **2023**, *410*, 135418.

(8) Priya, S.; Desai, V. M.; Singhvi, G. Surface Modification of Lipid-Based Nanocarriers: A Potential Approach to Enhance Targeted Drug Delivery. *ACS Omega* **2023**, *8* (1), 74−86.

(9) Qiu, C.; Julian McClements, D.; Jin, Z.; Qin, Y.; Hu, Y.; Xu, X.; Wang, J. Resveratrol-loaded core-shell nanostructured delivery systems: Cyclodextrin-based metal-organic nanocapsules prepared by ionic gelation. *Food Chem.* **2020**, *317*, 126328.

(10) Li, M.; Zhang, L.; Li, R.; Yan, M. New resveratrol micelle formulation for ocular delivery: characterization and in vitro/ in vivo evaluation. *Drug Dev. Ind. Pharm.* **2020**, *46* (12), 1960−1970.

(11) Vivero-Lopez, M.; Muras, A.; Silva, D.; Serro, A. P.; Otero, A.; Concheiro, A.; Alvarez-Lorenzo, C.; et al. Resveratrol-loaded hydrogel contact lenses with antioxidant and antibiofilm performance. *Pharmaceutics* **2021**, *13* (4), 532.

(12) Singh, G.; Pai, R. S. Trans-resveratrol self-nano-emulsifying drug delivery system (SNEDDS) with enhanced bioavailability potential: optimization, pharmacokinetics and in situ single pass intestinal perfusion (SPIP) studies. *Drug Delivery* **2015**, *22* (4), 522−530.

(13) Matos, M.; Gutiérrez, G.; Coca, J.; Pazos, C. Preparation of water-in-oil-in-water (W1/O/W2) double emulsions containing trans-resveratrol. *Colloids Surf., A* **2014**, *442*, 69−79.
(14) Ng, Y. J.; Benson, H. A. E.; Brown, D. H.; Chen, Y. Synthesis and characterization of novel copolymeric resveratrol conjugates. *J. Chem.* **2015**, *2015*, 245625.
(15) Muller, A. G.; Sarker, S. D.; Fatokun, A. A.; Hutcheon, G. A. Formulation of resveratrol into PGA-co-PDL nanoparticles increases its cytotoxic potency against lung cancer cells. *RPS Pharm. Pharmacol. Rep.* **2023**, *2* (1), rqac007.
(16) Nam, J.-B.; Ryu, J.-H.; Kim, J.-W.; Chang, I.-S.; Do, S.-K. Stabilization of resveratrol immobilized in monodisperse cyano-functionalized porous polymeric microspheres. *Polymer* **2005**, *46* (21), 8956−8963.
(17) Pereira, A. G.; Carpena, M.; Oliveira, P. G.; Mejuto, J. C.; Prieto, M. A.; Gandara, J. S. Main Applications of Cyclodextrins in the Food Industry as the Compounds of Choice to Form Host−Guest Complexes. *Int. J. Mol. Sci.* **2021**, *22* (3), 1339.
(18) Davis, M. E.; Brewster, M. E. Cyclodextrin-based pharmaceutics: past, present and future. *Nat. Rev. Drug Discovery* **2004**, *3* (12), 1023−1035.
(19) Amri, A.; Chaumeil, J. C.; Sfar, S.; Charrueau, C. Administration of resveratrol: What formulation solutions to bioavailability limitations? *J. Controlled Release* **2012**, *158* (2), 182−193.
(20) Das, S.; Lin, H. S.; Ho, P. C.; Ng, K. Y. The impact of aqueous solubility and dose on the pharmacokinetic profiles of resveratrol. *Pharm. Res.* **2008**, *25* (11), 2593−2600.
(21) Ansari, K. A.; Vavia, P. R.; Trotta, F.; Cavalli, R. Cyclodextrin-Based Nanosponges for Delivery of Resveratrol: *In Vitro* Characterisation, Stability, Cytotoxicity and Permeation Study. *AAPS PharmScitechnol* **2011**, *12* (1), 279.
(22) Pushpalatha, R.; Selvamuthukumar, S.; Kilimozhi, D. Cyclodextrin nanosponge based hydrogel for the transdermal co-delivery of curcumin and resveratrol: Development, optimization, in vitro and ex vivo evaluation. *J. Drug Delivery Sci. Technol.* **2019**, *52*, 55−64.
(23) Allan, K. E.; Lenehan, C. E.; Ellis, A. V. UV Light Stability of α-Cyclodextrin/Resveratrol Host-Guest Complexes and Isomer Stability at Varying pH. *Aust. J. Chem.* **2009**, *62* (8), 921−926.
(24) Rekharsky, M. V.; Inoue, Y. Complexation Thermodynamics of Cyclodextrins. *Chem. Rev.* **1998**, *98* (5), 1875−1917.
(25) Bertacche, V.; Lorenzi, N.; Nava, D.; Pini, E.; Sinico, C. Host-guest interaction study of resveratrol with natural and modified cyclodextrins. *J. Incl. Phenom. Macrocycl. Chem.* **2006**, *55* (3−4), 279−287.
(26) Joseph, A.; Balakrishnan, A.; Shanmughan, P.; Maliakel, B.; Illathu Madhavamenon, K. Micelle/Hydrogel Composite as a "Natural Self-Emulsifying Reversible Hybrid Hydrogel (N'SERH)" Enhances the Oral Bioavailability of Free (Unconjugated) Resveratrol. *ACS Omega* **2022**, *7* (15), 12835−12845.
(27) Joseph, A.; Kumar, D.; Balakrishnan, A.; Shanmughan, P.; Maliakel, B.; Krishnakumar, I. M. Surface-engineered liposomal particles of calcium ascorbate with fenugreek galactomannan enhanced the oral bioavailability of ascorbic acid: a randomized, double-blinded, 3-sequence, crossover study. *RSC Adv.* **2021**, *11* (60), 38161−38171.
(28) Perak Junaković, E.; Šandor, K.; Terzić, S.; Vujnović, A.; Andrišić, M.; Benić, M.; et al. Influence of Encapsulation of Propolis Extract with 2-Hydroxypropyl-β-cyclodextrin (HP-β-CD) on Polyphenolic Contents during *in Vitro* Simulation of Digestion. *Appl. Sci. (Switzerland)* **2023**, *13* (16), 9357.
(29) ICH Topic Q 1 A (R2) Stability Testing of new Drug Substances and Products, 2003. https://www.ema.europa.eu/en/documents/scientific-guideline/ich-q-1-r2-stability-testing-new-drug-substances-products-step-5_en.pdf.
(30) Zhang, Y.; Barringer, S. Effect of hydrocolloids, sugar, and citric acid on strawberry volatiles in a gummy candy. *J. Food Process. Preserv.* **2018**, *42* (1), No. e13327.
(31) Orgulloso-Bautista, S.; Ortega-Toro, R.; García Zapateiro, L. A. Design and Application of Hydrocolloids from Butternut Squash (*Cucurbita moschata*) Epidermis as a Food Additive in Mayonnaise-type Sauces. *ACS Omega* **2021**, *6* (8), 5499−5508.
(32) Mahapatra, A. K.; Murthy, P. N.; Swain, R. P.; Sravani, Y.; Sagar, G. Sustained Release Products: A Review on Formulation Technologies and Regulatory Aspects. *Res. J. Pharm. Technol.* **2013**, *6* (12), 1415−1425.
(33) Kaur, G.; Grewal, J.; Jyoti, K.; Jain, U. K.; Chandra, R.; Madan, J. Oral controlled and sustained drug delivery systems: Concepts, advances, preclinical, and clinical status. *Drug Targeting Stimuli Sensitive Drug Delivery Syst.* **2018**, 567−626.
(34) Khorshidian, N.; Yousefi Asli, M.; Arab, M.; Adeli Mirzaie, A.; Mortazavian, A. M. Fenugreek: Potential Applications as a Functional Food and Nutraceutical. *Nutr. Food Sci. Res.* **2016**, *3* (1), 5−16.
(35) Amri, S.; Chaumeil, J. C.; Sfar, S.; Charrueau, C. Administration of resveratrol: What formulation solutions to bioavailability limitations? *J. Controlled Release* **2012**, *158* (2), 182−193.
(36) Lopez-Nicolas, J. M.; Bru, R.; Sanchez-Ferrer, A.; Garcia-Carmona, F. Use of 'soluble lipids' for biochemical processes: linoleic acid-cyclodextrin inclusion complexes in aqueous solutions. *Biochem. J.* **1995**, *308* (1), 151−154.
(37) Matencio, A.; García-Carmona, F.; López-Nicolás, J. M. Encapsulation of piceatannol, a naturally occurring hydroxylated analogue of resveratrol, by natural and modified cyclodextrins. *Food Funct.* **2016**, *7* (5), 2367−2373.
(38) Zupančič, Š; Lavrič, Z.; Kristl, J. Stability and solubility of trans-resveratrol are strongly influenced by pH and temperature. *Eur. J. Pharm. Biopharm.* **2015**, *93*, 196−204.
(39) Wu, K.; Zhang, T.; Chai, X.; Duan, X.; He, D.; Yu, H.; et al. Encapsulation Efficiency and Functional Stability of Cinnamon Essential Oil in Modified β-cyclodextrins: *In Vitro* and in Silico Evidence. *Foods* **2023**, *12* (1), 45.
(40) Joye, I. J.; Davidov-Pardo, G.; Ludescher, R. D.; McClements, D. J. Fluorescence quenching study of resveratrol binding to zein and gliadin: Towards a more rational approach to resveratrol encapsulation using water-insoluble proteins. *Food Chem.* **2015**, *185*, 261−267.
(41) Mohandoss, S.; Atchudan, R.; Edison, T. N. J. I.; Mishra, K.; Tamargo, R. J. I.; Palanisamy, S.; Yelithao, K.; You, S.; Napoleon, A. A.; Lee, Y. R. Enhancement of solubility, antibiofilm, and antioxidant activity of uridine by inclusion in β-cyclodextrin derivatives. *J. Mol. Liq.* **2020**, *306*, 112849.
(42) Ying, M.; Huang, F.; Ye, H.; Xu, H.; Shen, L.; Huan, T.; et al. Study on interaction between curcumin and pepsin by spectroscopic and docking methods. *Int. J. Biol. Macromol.* **2015**, *79*, 201−208.
(43) Joseph, A.; Shanmughan, P.; Balakrishnan, A.; Maliakel, B.; Krishnakumar, I. M. Enhanced Bioavailability and Pharmacokinetics of a Natural Self-Emulsifying Reversible Hybrid-Hydrogel System of Quercetin: A Randomized Double-Blinded Comparative Crossover Study. *ACS Omega* **2022**, *7* (50), 46825−46832.
(44) Shah, A. A.; Shah, A.; Lewis, S.; Ghate, V.; Saklani, R.; Narayana Kalkura, S.; Baby, C.; Singh, P. K.; Nayak, Y.; Chourasia, M. K. Cyclodextrin based bone regenerative inclusion complex for resveratrol in postmenopausal osteoporosis. *Eur. J. Pharm. Biopharm.* **1721**, *167*, 127−139.
(45) Lu, Z.; Chen, R.; Liu, H.; Hu, Y.; Cheng, B.; Zou, G. Study of the complexation of resveratrol with cyclodextrins by spectroscopy and molecular modeling. *J. Incl. Phenom. Macrocycl. Chem.* **2009**, *63* (3−4), 295−300.
(46) Goswami, S.; Sarkar, S. M. Fluorescence, FTIR and 1 H NMR studies of the inclusion complexes of the painkiller lornoxicam with β-, γ-cyclodextrins and their hydroxy propyl derivatives in aqueous solutions at different pHs and in the solid state. *New J. Chem.* **2018**, *42* (18), 15146−15156.
(47) Xiong, W.; Ren, C.; Li, J.; Li, B. Enhancing the photostability and bioaccessibility of resveratrol using ovalbumin−carboxymethylcellulose nanocomplexes and nanoparticles. *Food Funct.* **2018**, *9* (7), 3788−3797.

https://doi.org/10.1021/acsomega.3c09828
ACS Omega 2024, 9, 35275−35286

(48) Aytac, Z.; Celebioglu, A.; Yildiz, Z. I.; Uyar, T. Efficient Encapsulation of Citral in Fast-Dissolving Polymer-Free Electrospun Nanofibers of Cyclodextrin Inclusion Complexes: High Thermal Stability, Longer Shelf-Life, and Enhanced Water Solubility of Citral. *Nanomaterials (Basel)* **2018**, *8* (10), 793.
(49) Sambasevam, K. P.; Mohamad, S.; Sarih, N. M.; Ismail, N. A. Synthesis and Characterization of the Inclusion Complex of β-cyclodextrin and Azomethine. *Int. J. Mol. Sci.* **2013**, *14* (2), 3671−3682.
(50) Issarani, R.; Nagori, B. P. FTIR-Spectrum of Galactomannan Extracted from Trigonella Foenum - Graceum. *Indian J. Pharm. Sci.* **2004**, *66* (3), 358−360.
(51) Bouaziz, F.; Koubaa, M.; Barba, F. J.; Roohinejad, S.; Chaabouni, S. E. Antioxidant Properties of Water-Soluble Gum from Flaxseed Hulls. *Antioxidants* **2016**, *5* (3), 26.
(52) Selvaraj, S.; Duraipandy, N.; Kiran, M. S.; Fathima, N. N. Antioxidant enriched hybrid nanofibers: Effect on mechanical stability and biocompatibility. *Int. J. Biol. Macromol.* **2018**, *117*, 209−217.
(53) Dhull, S. B.; Sandhu, K. S.; Punia, S.; Kaur, M.; Chawla, P.; Malik, A. Functional, thermal and rheological behavior of fenugreek (*Trigonella foenum-graecum* L.) gums from different cultivars: A comparative study. *Int. J. Biol. Macromol.* **2020**, *159*, 406−414.
(54) Lu, J.; Shin, I. D.; Nojima, S.; Tonelli, A. E. Formation and characterization of the inclusion compounds between poly(ε-caprolactone)-poly(ethylene oxide)-poly(ε-caprolactone) triblock copolymer and α- and γ-cyclodextrin. *Polymer* **2000**, *41* (15), 5871−5883.
(55) Silva, A. F. R.; Monteiro, M.; Resende, D.; Braga, S. S.; Coimbra, M. A.; Silva, A. M. S.; et al. Inclusion Complex of Resveratrol with γ-Cyclodextrin as a Functional Ingredient for Lemon Juices. *Foods* **2021**, *10* (1), 16.
(56) Kayaci, F.; Uyar, T. Solid inclusion complexes of vanillin with cyclodextrins: Their formation, characterization, and high-temperature stability. *J. Agric. Food Chem.* **2011**, *59* (21), 11772−11778.
(57) Li, H.; Chang, S.-L.; Chang, T.-R.; You, Y.; Wang, X.-D.; Wang, L.-W.; Yuan, X.-F.; Tan, M.-H.; Wang, P.-D.; Xu, P.-W.; et al. Inclusion complexes of cannabidiol with β-cyclodextrin and its derivative: Physicochemical properties, water solubility, and antioxidant activity. *J. Mol. Liq.* **2021**, *334*, 116070.
(58) Wang, Y.; Yan, M.; Xu, L.; Zhao, W.; Wang, X.; Dong, S.; et al. Aptamer-functionalized DNA microgels: a strategy towards selective anticancer therapeutic systems. *J. Mater. Chem. B* **2016**, *4* (32), 5446−5454.
(59) Caccavo, D.; Cascone, S.; Lamberti, G.; Barba, A. A. Modeling the drug release from hydrogel-based matrices. *Mol. Pharm.* **2015**, *12* (2), 474−483.
(60) Hao, X.; Sun, X.; Zhu, H.; Xie, L.; Wang, X.; Jiang, N.; Fu, P.; Sang, M.; et al. Hydroxypropyl-β-Cyclodextrin-Complexed Resveratrol Enhanced Antitumor Activity in a Cervical Cancer Model: *In Vivo* Analysis. *Front. Pharmacol.* **2021**, *12*, 573909.
(61) Morais, D. C.; Fontes, M. L.; Oliveira, A. B.; Gabbai-Armelin, P. R.; Ferrisse, T. M.; De Oliveira, L. F. C.; et al. Combining Polymer and Cyclodextrin Strategy for Drug Release of Sulfadiazine from Electrospun Fibers. *Pharmaceutics* **2023**, *15* (7), 1890.

https://doi.org/10.1021/acsomega.3c09828
ACS Omega 2024, 9, 35275−35286